Planetary and Space Science 58 (2010) 1425–1433

Contents lists available at ScienceDirect

Planetary and Space Science

journal homepage: www.elsevier.com/locate/pss

Standing slow magnetosonic waves in a dipole-like plasmasphere

A.S. Leonovich *, D.A. Kozlov, I.K. Edemskiy

Institute of Solar-Terrestrial Physics SB RAS, P.O. Box 291, Irkutsk 664033, Russia

ARTICLE INFO

Article history:
Received 16 March 2010
Received in revised form
11 June 2010
Accepted 14 June 2010
Available online 16 June 2010

Keywords:
Magnetosphere
MHD-oscillations
Theory

ABSTRACT

A problem of the structure and spectrum of standing slow magnetosonic waves in a dipole plasmasphere is solved. Both an analytical (in WKB approximation) and numerical solutions are found to the problem, for a distribution of the plasma parameters typical of the Earth's plasmasphere. The solutions allow us to treat the total electronic content oscillations registered above Japan as oscillations of one of the first harmonics of standing slow magnetosonic waves. Near the ionosphere the main components of the field of registered standing SMS waves are the plasma oscillations along magnetic field lines, plasma concentration oscillation and the related oscillations of the gas-kinetic pressure. The velocity of the plasma oscillations increases dramatically near the ionospheric conductive layer, which should result in precipitation of the background plasma particles. This may be accompanied by ionospheric F2 region airglows modulated with the periods of standing slow magnetosonic waves.

1. Introduction

Electromagnetic oscillations of planets' magnetospheres in the low-frequency part of the spectrum are MHD waves. The typical spatial scales of most low-frequency MHD oscillations are comparable with the magnetospheric scales. There are two modes of MHD oscillations capable of propagating almost exactly along magnetic field lines—the Alfven waves and slow magnetosonic (SMS) waves. Propagation of the fast magnetosonic (FMS) waves is not related to the magnetic field direction. Since magnetic field lines are closed, they cross the ionosphere twice (in the case of the Earth—in the Northern and Southern hemispheres). Because it is highly conductive, the ionosphere is an almost ideally reflecting boundary for the waves under consideration. Therefore the Alfven and SMS oscillations can form standing (along magnetic field lines) waves in the magnetosphere. Many papers have been devoted to the structure and spectrum of the standing Alfven waves in dipole-like model magnetospheres (see Radoski, 1967; Cummings et al., 1969; Leonovich and Mazur, 1989; Chen and Cowley, 1989; Lee and Lysak, 1991; Wright, 1992 etc.).

Meanwhile, investigations of standing SMS waves are fairly few: Taylor and Walker (1987), Leonovich et al. (2006), and Klimushkin and Mager (2008). Insufficient attention paid to the waves is probably due to their rather large decrement (Leonovich and Kozlov, 2009), thanks to which the eigen-SMS-oscillations decay rapidly making them difficult to register. Nevertheless, if there is a rather strong source capable of generating such waves, they may well be observed in the magnetosphere. Resonant SMS waves excited in a dipole magnetosphere by a monochromatic fast magnetosonic wave penetrating from the solar wind into the magnetosphere were studied in Leonovich et al. (2006). The typical wavelength of such SMS oscillations both in the direction along magnetic field lines and in the azimuthal direction is of the order of the characteristic scale of magnetospheric plasma inhomogeneity. Across the magnetic shells, they have a typical resonance structure with a characteristic scale that is much smaller than the scale of magnetospheric plasma inhomogeneity. Their amplitude decreases dramatically from the magnetospheric equatorial plane to the ionosphere. Therefore, such oscillation is possible to register at high-orbit spacecraft only.

Total electronic content (TEC) oscillations were registered by Afraimovich et al. (2009) in GPS observations over Japan concerning the terminator transit over the Earth's ionosphere in regions connected with the observation region through the geomagnetic field lines. Such oscillations are best registered at times close to the summer solstice. The oscillations appear in the ionospheric region under consideration 20–30 min after the evening terminator passes over the magnetoconjugated region of the Southern hemisphere. The terminator passes through the observation regions only 1 h after the TEC oscillations start. Since the terminator at the latitudes under consideration moves at supersonic velocity, the ÒÅÑ oscillations in the period in question cannot be related to the inner gravity waves generated by the terminator. These waves are most likely responsible for the oscillations of the total electronic content after the terminator passes over the observation point. The periods of the observed

* Corresponding author. Tel.: +7 89148979925; fax: +7 83952511675.
E-mail address: leon@iszf.irk.ru (A.S. Leonovich).

0032-0633/$ - see front matter © 2010 Elsevier Ltd. All rights reserved.
doi:10.1016/j.pss.2010.06.007

TEC oscillations were within the 15–30 min range. Lower-frequency oscillations were filtered artificially so as to eliminate the effect of the GPS satellite movement.

Thus, a relationship is clearly traceable between the TEC oscillations and processes in the magnetoconjugate region of the ionosphere. Therefore it was suggested that the magnetoconjugate regions of the ionosphere interact through the Alfven or SMS waves moving along the geomagnetic field lines. Both these wave types are capable of disturbing the electron concentration near the ionosphere. The disturbance of the concentration is an essential property of the SMS waves. Whereas the Alfven waves can disturb the concentration when they impinge onto the ionosphere, by generating a FMS oscillation in the ionospheric conducting layer (Pilipenko and Fedorov, 1995).

However, the specific periods of the first harmonics of standing Alfven waves at the magnetic shells under consideration (~ 10 s) are very far from the periods of the observed TEC oscillations. Therefore the generation of the observable oscillations by the Alfven wave appears to be ineffective. The periods of the first harmonics of standing SMS waves (~ 20 min) fit exactly in the required range. Therefore the conclusion has been made in Afraimovich et al. (2009) that the TEC oscillations related to the terminator transit in the magnetoconjugated region of the ionosphere are, in fact, one (or a few) of the first harmonics of standing SMS waves.

The assumption was based on the periods of the several first harmonics of these oscillations as calculated in the WKB approximation. More rigorous substantiation is needed, however. For the purpose, we will calculate the total field of standing SMS waves in the dipole model of the Earth's plasmasphere and compare the results with the observational data. SMS waves related to the terminator transit are likely to have a rather large typical wavelength across magnetic shells (comparable with the typical scale of magnetospheric inhomogeneity) while being fairly small-scale in the azimuthal direction. This paper is devoted to calculating the spectrum, structure and amplitude of the wave field components of such azimuthally small-scale standing SMS waves observed near the ionosphere. The calculations are done both analytically—in the WKB approximation—and numerically. The results of the analytical calculations are compared to the numerical results, and both these results are also compared to observational data.

This paper has the following structure. Section 2 deals with describing the model medium, deriving the basic equation for calculating the structure and spectrum of azimuthally small-scale standing SMS waves as well as obtaining analytical expressions for the oscillation field components. An analytical WKB solution to the basic equation describing the structure of the oscillation field along a magnetic field line is obtained in Section 3. A numerical solution to the basic equation is found, the distributions of the oscillation field components along a magnetic field line are constructed and the results are discussed in Section 4. The Conclusion lists the main results of the paper.

2. The model medium and the basic equations

Let us consider a model plasmasphere with dipole-like magnetic field in Fig. 1. Let us introduce a curvilinear orthogonal coordinate system (x^1,x^2,x^3) associated with the magnetic field lines. The x^3 coordinate is directed along the field line, x^1 across the magnetic shells, and x^2 makes the coordinates system a right-handed one. The square of the length element in this coordinate system is determined as

$$ds^2 = g_1(dx^1)^2 + g_2(dx^2)^2 + g_3(dx^3)^2,$$

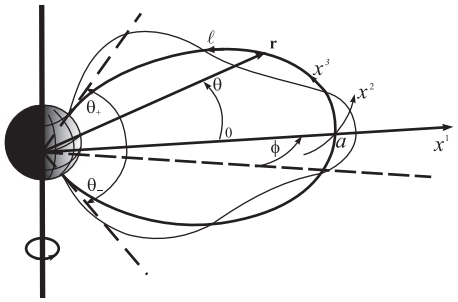

Fig. 1. The curvilinear orthogonal coordinate system (x^1,x^2,x^3) associated with magnetic field lines and the nonorthogonal coordinate system (a,ϕ,θ) used in numerical calculations. The structure of the fifth harmonic of standing SMS-waves along a magnetic field line is shown schematically.

where g_1,g_2,g_3 are the metric tensor components of the curvilinear coordinate system under study. Let us assume the plasma and magnetic field to be homogeneous with respect to the x^2 coordinate. We will describe the MHD oscillations using the equation system for the ideal MHD:

$$\rho\frac{d\mathbf{v}}{dt} = -\nabla P + \frac{1}{4\pi}[\mathrm{curl}\,\mathbf{B}\times\mathbf{B}], \tag{1}$$

$$\frac{\partial\mathbf{B}}{\partial t} = \mathrm{curl}[\mathbf{v}\times\mathbf{B}], \tag{2}$$

$$\frac{\partial\rho}{\partial t} + \nabla(\rho\mathbf{v}) = 0, \tag{3}$$

$$\frac{d}{dt}\frac{P}{\rho^\gamma} = 0, \tag{4}$$

where $\mathbf{B}$ and $\mathbf{v}$ are the magnetic field intensity and plasma motion velocity vectors, respectively, ρ and P are the plasma density and pressure, γ is the adiabatic index. Moreover, we will determine the oscillation electric field $\mathbf{E}$ using the drift approximation

$$\mathbf{E} = -\frac{[\mathbf{v}\times\mathbf{B}]}{c}.$$

In steady state ($\partial/\partial t = 0$) the system (1)–(4) describes the distribution of parameters of an unperturbed magnetosphere: $\mathbf{B_0},\mathbf{v_0}$, $\mathbf{E_0},\rho_0,P_0$. We will assume the plasma to be immobile ($\mathbf{v_0} = \mathbf{E_0} = 0$). Let us linearize the system (1)–(4) with respect to small disturbances: $\mathbf{B} = \mathbf{B_0} + \tilde{\mathbf{B}}$, $\mathbf{v} = \mathbf{v_0} + \tilde{\mathbf{v}}, \mathbf{E} = \tilde{\mathbf{E}}, \rho = \rho_0 + \tilde{\rho}$, $P = P_0 + \tilde{P}$, where $\tilde{\mathbf{B}},\tilde{\mathbf{v}},\tilde{\mathbf{E}},\tilde{\rho},\tilde{P}$ are the field components related to the plasma MHD oscillations. Let us present each disturbed component as an expansion over the Fourier harmonics of the form $\exp(ik_2x^2 - i\omega t)$, where ω is the oscillation frequency, k_2 is the azimuthal wave number (if $x^2 \equiv \phi$ is the azimuthal angle, $k_2 \equiv m = 1,2,3,\ldots$). From (1) we have

$$-i\omega\rho_0 v_1 = -\nabla_1\tilde{P} + \frac{B_0}{4\pi}\frac{1}{\sqrt{g_3}}(\nabla_3 B_1 - \nabla_1 B_3), \tag{5}$$

$$-i\omega\rho_0 v_2 = -ik_2\tilde{P} - \frac{B_0}{4\pi}\frac{1}{\sqrt{g_3}}(ik_2 B_3 - \nabla_3 B_2), \tag{6}$$

$$i\omega\rho_0 v_3 = \nabla_3\tilde{P}, \tag{7}$$

where v_i,B_i $(i = 1,2,3)$ are the covariant components of the disturbed velocity $\tilde{\mathbf{v}}$ and magnetic field $\tilde{\mathbf{B}}$ vectors, $\nabla_i \equiv \partial/\partial x^i$. From (3), (4) we obtain

$$\tilde{P} = -i\frac{\gamma}{\omega}\frac{P_0^{1-\sigma}}{\sqrt{g}}\left[\nabla_1\left(\frac{\sqrt{g}}{g_1}P_0^\sigma v_1\right) + ik_2\frac{\sqrt{g}}{g_2}P_0^\sigma v_2 + \nabla_3\left(\frac{\sqrt{g}}{g_3}P_0^\sigma v_3\right)\right],$$

where $g = \sqrt{g_1 g_2 g_3}$, $\sigma = 1/\gamma$.

In order to describe the MHD oscillation field it is convenient to use potentials instead of the field oscillation components $\tilde{\mathbf{B}},\tilde{\mathbf{v}},\tilde{\mathbf{E}},\tilde{\rho},\tilde{P}$. The Helmholtz expansion theorem (Korn and Korn, 1968) allows an arbitrary vector field at each point of which its first derivative is determined to be represented as the sum of the potential and vortex fields. For a two-dimensional (2-D) vector field $\tilde{\mathbf{E}}=(E_1,E_2,0)$ this expansion has the form:

$$\tilde{\mathbf{E}}=-\nabla_\perp\varphi+[\nabla_\perp,\boldsymbol{\Psi}],$$

where $\nabla_\perp\equiv(\nabla_1,\nabla_2)$, φ is the scalar potential, and $\boldsymbol{\Psi}$ is the vector potential.

An appropriate calibration can be used to make the vector potential have only one, longitudinal, component: $\boldsymbol{\Psi}=(0,0,\psi_3\equiv\psi)$. Using a linearized system (1)–(4) it is possible to express the components of a perturbed field through the potentials φ and ψ:

$$E_1=-\nabla_1\varphi+ik_2\psi, \tag{8}$$

$$E_2=-ik_2\varphi-\nabla_1\psi, \tag{9}$$

$$E_3=0, \tag{10}$$

$$B_1=\frac{c}{\omega}\frac{g_1}{\sqrt{g}}\nabla_3\left(k_2\varphi-i\frac{g_2}{\sqrt{g}}\nabla_1\psi\right),$$

$$B_2=\frac{c}{\omega}\frac{g_2}{\sqrt{g}}\nabla_3\left(i\nabla_1\varphi+k_2\frac{g_1}{\sqrt{g}}\psi\right), \tag{11}$$

$$B_3=i\frac{c}{\omega}\frac{g_3}{\sqrt{g}}\left(\nabla_1\frac{g_2}{\sqrt{g}}\nabla_1\psi-k_2^2\frac{g_1}{\sqrt{g}}\psi\right),$$

$$v_1=-\frac{cp^{-1}}{B_0}\left(ik_2\varphi+\frac{g_2}{\sqrt{g}}\nabla_1\psi\right),$$

$$v_2=\frac{cp}{B_0}\left(\nabla_1\varphi-ik_2\frac{g_1}{\sqrt{g}}\psi\right), \tag{12}$$

$$v_3=-i\frac{\nabla_3\tilde{P}}{\omega\rho_0}, \tag{13}$$

and we obtain an equation for disturbed pressure

$$\hat{L}_0\tilde{P}=i\gamma\frac{c}{\omega}\frac{P_0^{1-\sigma}}{\sqrt{g}}\left[ik_2\varphi\nabla_1\frac{\sqrt{g_3}P_0^\sigma}{B_0}.+\nabla_1\frac{pP_0^\sigma}{B_0}\nabla_1\psi-k_2^2\frac{p^{-1}P_0^\sigma}{B_0}\psi\right], \tag{14}$$

where $p=\sqrt{g_2/g_1}$,

$$\hat{L}_0=\frac{\gamma}{\omega^2}\frac{P_0^{1-\sigma}}{\sqrt{g}}\nabla_3\frac{\sqrt{g}}{g_3}\frac{P_0^\sigma}{\rho_0}\nabla_3+1.$$

Let us multiply (5) by ik_2B_0/ρ_0, (6) by B_0/ρ_0, differentiate with respect to x^1 and subtract one obtained equation from the other. The result will be

$$\nabla_1\hat{L}_T\nabla_1\varphi-k_2^2\left(\hat{L}_P\varphi+\frac{S^2}{A^2}\frac{\varphi}{\sqrt{g_1g_2}}\nabla_1\ln B_0\nabla_1\ln\frac{\sqrt{g_3}P_0^\sigma}{B_0}\right)$$
$$=i\frac{k_2}{\omega}\left(\nabla_1\hat{L}_T\frac{g_1}{\sqrt{g}}\psi-\hat{L}_P\frac{g_2}{\sqrt{g}}\nabla_1\psi\right), \tag{15}$$

where

$$\hat{L}_T=\frac{1}{\sqrt{g_3}}\nabla_3\frac{p}{\sqrt{g_3}}\nabla_3+p\frac{\omega^2}{A^2},$$

$$\hat{L}_P=\frac{1}{\sqrt{g_3}}\nabla_3\frac{p^{-1}}{\sqrt{g_3}}\nabla_3+p^{-1}\frac{\omega^2}{A^2},$$

are the toroidal and poloidal longitudinal operators, $S=\gamma\sqrt{P_0/\rho_0}$ is the sound velocity in plasma, $A=B_0/\sqrt{4\pi\rho_0}$ is the Alfven speed. Let us act the $\hat{L}_0$ functional on (6) and substitute the components of the disturbed field from (10)–(13) into the resulting equation. After some regrouping, we obtain

$$\frac{B_0\sqrt{g_3}}{4\pi\rho_0}\hat{L}_0\frac{B_0}{\sqrt{g_3}}\tilde{\Delta}\psi+S^2\overline{\Delta}\psi+\omega^2\psi=$$
$$-i\frac{B_0\sqrt{g_3}}{4\pi k_2\rho_0}\hat{L}_0B_0\hat{L}_T\nabla_1\varphi-i\varphi k_2S^2\frac{g_3}{\sqrt{g}}\nabla_1\ln\frac{\sqrt{g_3}P_0^\sigma}{B_0}, \tag{16}$$

where

$$\tilde{\Delta}=\frac{g_3}{\sqrt{g}}\nabla_1\frac{g_2}{\sqrt{g}}\nabla_1-\frac{k_2^2}{g_2}+\nabla_3\frac{g_2}{\sqrt{g}}\nabla_3\frac{g_1}{\sqrt{g}},$$

$$\overline{\Delta}=\frac{B_0}{P_0^\sigma}\frac{1}{\sqrt{g_1g_2}}\left(\nabla_1\frac{pP_0^\sigma}{B_0}\nabla_1-\frac{k_2^2}{p}\frac{P_0^\sigma}{B_0}+\nabla_3\frac{\sqrt{g}}{g_3}\frac{P_0^\sigma}{\rho_0}\nabla_3\frac{\rho_0}{B_0\sqrt{g_3}}\right),$$

are Laplacian analogues. Eqs. (15) and 16 formed a set of equations closed with respect to potentials φ and ψ. The right sides in (15) and (16) tend to zero when we pass to homogeneous plasma. The functional in the left side of (15) yields a dispersion equation for the Alfven waves $\omega^2=k_\parallel^2A^2$, where $k_\parallel^2\equiv k_3^2/g_3$, while the operator in the left side of (16) yields a dispersion equation for the magnetosonic waves:

$$\omega^4-\omega^2k^2(A^2+S^2)+k^2k_\parallel^2A^2S^2=0, \tag{17}$$

where $k^2=k_\parallel^2+k_\perp^2$, $k_\perp^2=k_1^2/g_1+k_2^2/g_2$. Therefore, it is justified to conclude that the Alfven oscillations are described by the scalar potential φ, and the magnetosonic waves by the longitudinal component of the vector potential ψ. In an inhomogeneous plasma the right sides of (15) and (16) describe coupling of these branches of MHD oscillations. A solution to (17) may be presented in the form:

$$\omega^2=\frac{k^2}{2}(A^2+S^2)\pm\sqrt{\frac{k^4}{4}(A^2+S^2)^2-k^2k_\parallel^2A^2S^2}.$$

The plus sign corresponds to a dispersion equation for FMS waves, whereas the minus sign to a dispersion equation for SMS waves. If one of the inequalities $S\ll A$, $A\ll S$, $|k_\parallel|\ll|k_\perp|$ is valid, it is possible to obtain the following approximate dispersion equations:

$$\omega^2\approx k^2C_F^2,$$

–for FMS-waves, where $C_F^2=A^2+S^2$, and

$$\omega^2\approx k_\parallel^2C_S^2,$$

– for SMS-waves, where $C_S^2=A^2S^2/(A^2+S^2)$. One can see from the form of these dispersion equations that C_F and C_S are the phase velocities of the FMS and SMS wave, respectively. The numerical calculations to follow rely on using the numerical Krinberg–Tashchilin model plasmasphere, presented in detail in Krinberg and Taschilin (1984) to calculate the distribution of parameters of background plasma along a magnetic field line. Fig. 2 presents the distribution the Alfven speed A and the velocity of SMS waves C_S along the magnetic field line crossing the Earth's ionosphere over Japan (37°N, 138°E) for June 14, 2008, at 11 h UT. One can see that at least one of the above inequalities ($S\ll A$) holds practically for the entire length of the field line. The parameters of the medium in the Northern and Southern hemispheres were calculated from 80 km altitude up to the field-line top point $\sim$1700 km. Let us take a special note of the sharp increase of A and the decrease of C_s for altitudes $h<400$ km. They are due, respectively, to a sharply decreasing concentration and temperature of plasma ions at altitudes below the ionospheric F2-layer. The strong asymmetry in the A and C_s profiles in the Northern and Southern hemisphere is caused by differing boundary conditions on the ionospheric ends of the field line: the ionosphere in the Northern hemisphere is illuminated by the Sun, while being already in the shades in the Southern hemisphere.

In this approximation the dispersion equation for SMS waves is very similar to the dispersion equation for Alfven waves. The

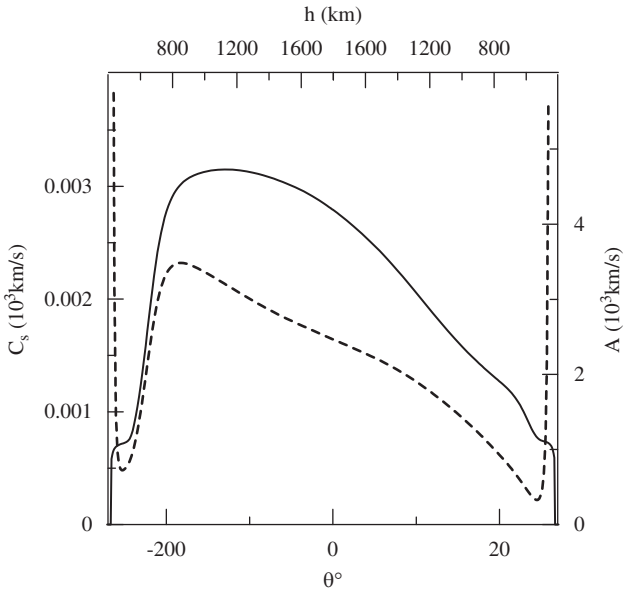

Fig. 2. Alfven speed $A(\theta)$ (dashed line) and SMS wave velocity $C_s(\theta)$ distributions (solid line) along the field line crossing the Earth's ionosphere in the Northern hemisphere above Japan (37°N, 138°E) at 11 h UT on June 14, 2008. The parameters of the medium were calculated using the numerical model of the plasmasphere by Krinberg and Taschilin (1984).

velocity of SMS waves, as well as the Alfven speed, is directed along the magnetic field lines. Since the potential ψ describes both the fast and the slow magnetosonic waves, it is possible to represent it in the linear approximation as a sum $\psi=\psi_F+\psi_S$ where the ψ_F component refers to the FMS wave, and the ψ_S component to the SMS wave. It is possible to demonstrate that in homogeneous plasma the following relations are valid for SMS waves ($\varphi=0$, $\psi=\psi_S$)

$$(\tilde{P}+P_m)/\tilde{P}\sim(\tilde{P}+P_m)/P_m=\frac{k_\parallel^2}{k^2}\frac{A^2}{A^2+S^2},$$

where $P_m=B_0B_\parallel/4\pi$ is disturbed magnetic pressure. It follows from here that, for the oscillations with $k_\perp\gg k_\parallel$, the total pressure in the SMS wave is practically not disturbed:

$$\tilde{P}+\frac{B_0B_\parallel}{4\pi}\approx 0. \tag{18}$$

In the frame of the magnetospheric model under consideration, the typical eigenfrequencies of the first harmonics of standing Alfven and SMS waves differ by more than two orders of magnitudes. This means that coupling of the Alfven and SMS waves on the closed field lines is almost zero. Therefore, when studying the structure of the SMS oscillations described by (16), let us assume $\varphi=0$ in its right side. For FMS waves with periods >10 min, examined in this work, the entire magnetosphere is an opacity region. Therefore, we will assume that the FMS waves from the solar wind do not penetrate into the plasmasphere and $\psi_F=0$. For SMS waves in the plasmasphere we use (16) to obtain

$$\frac{B_0\sqrt{g_3}}{4\pi\rho_0}\hat{L}_0\frac{B_0}{\sqrt{g_3}}\tilde{\Delta}\psi_S+S^2\overline{\Delta}\psi_S+\omega^2\psi_S=0. \tag{19}$$

The boundary condition for the function ψ_S on the ionosphere was obtained in Leonovich et al. (2006). Vertical motions of the atmosphere disturb the ionospheric conducting layer and generate external currents $\mathbf{j}^{(ext)}$ in it. The boundary condition for the function ψ_S is

$$\psi_S|_{x^3=x^3_-}=i\frac{J^{(-)}}{\Sigma_P^{(-)}}, \tag{20}$$

where the x^3_- coordinate corresponds to the intersection point of a field line with the Southern ionosphere, $\Sigma_P^{(-)}$ is the height-integrated Pedersen conductivity of the ionosphere, and the functions $J^{(-)}\equiv J(x^3=x^3_-)$ are related to the density of external currents as follows:

$$\Delta_\perp J=\int_0^\Delta(\nabla\times\mathbf{j}^{(ext)})_z\,dz,$$

where $\Delta_\perp=\nabla_x^2+\nabla_y^2$ is the transverse Laplacian, Δ is the thickness of the ionospheric conducting layer.

The characteristic scales of the first harmonics of standing SMS waves excited by the terminator transit over the ionosphere, in a direction along magnetic field lines (over the x^3 coordinate) and across magnetic shells (over the x^1 coordinate), are much larger than their azimuthal scale (over the x^2 coordinate), determined by the width of the terminator front. Therefore, the method of various scales may be applied to finding a solution to (19). In the main order, (19) retaining the terms proportional to the large azimuthal wave number k_2 (determined as the value inverse to the azimuthal wavelength) only yields

$$\frac{S^2A^2}{\omega^2}\frac{\rho_0\sqrt{g_3}}{P_0^\sigma\sqrt{g}B_0}\nabla_3\frac{\sqrt{g}P_0^\sigma}{g_3\rho_0}\nabla_3\frac{B_0}{g_2\sqrt{g_3}}\psi_S+\frac{A^2+S^2}{g_2}\psi_S=0. \tag{21}$$

The solution to this equation may be written as

$$\psi_S=V(x^1)S(x^1,x^3),$$

where the function $V(x^1)$ is determined by the source of oscillations under consideration and describes the distribution of their amplitude across the magnetic shells. The function $S(x^1,x^3)$ describes the potential distribution ψ_S along a magnetic field line and is determined by Eq. (21). The function depends on the x^1 coordinate as a parameter. In further calculations it is convenient to introduce the function $H(x^1,x^3)=S(x^1,x^3)B_0/(g_2\sqrt{g_3})$ described by the equation

$$\frac{\partial}{\partial\ell}\alpha(x^1,\ell)\frac{\partial H}{\partial\ell}+\frac{\omega^2}{C_S^2}\alpha(x^1,\ell)H=0, \tag{22}$$

where $\partial\ell=\sqrt{g_3}\partial x^3$ is the length element along a field line (see Fig. 1), $\alpha(x^1,\ell)=P_0^\sigma\sqrt{g_1g_2}/\rho_0$. The main field components of azimuthally small-scale SMS waves may be represented in the form

$$E_1=ik_2\psi_S, \tag{23}$$

$$E_2=-\nabla_1\psi_S, \tag{24}$$

$$E_3=0, \tag{25}$$

$$B_1=-i\frac{c}{\omega}\frac{g_1}{\sqrt{g}}\nabla_3\frac{g_2}{\sqrt{g}}\nabla_1\psi_S, \tag{26}$$

$$B_2=k_2\frac{c}{\omega}\frac{g_2}{\sqrt{g}}\nabla_3\frac{g_1}{\sqrt{g}}\psi_S,$$

$$B_3=-i\frac{c}{\omega}\frac{k_2^2}{g_2}\psi_S, \tag{27}$$

$$v_1=-\frac{c}{B_0\sqrt{g_3}}\nabla_1\psi_S, \tag{28}$$

$$v_2=-i\frac{k_2c}{B_0\sqrt{g_3}}\psi_S, \tag{29}$$

$$v_3=-i\frac{\nabla_3\tilde{P}}{\omega\rho_0}. \tag{30}$$

In determining the disturbed pressure, let us use an approximate Eq. (18), which together with (27) and (29) yields the following expression for the longitudinal component of the plasma

oscillation velocity

$$v_{\parallel} \equiv \frac{v_3}{\sqrt{g_3}} \approx V(x^1)\frac{ck_2^2}{4\pi\rho_0\omega^2}\frac{\partial H(x^1,\ell)}{\partial \ell}. \quad (31)$$

As will be seen in the subsequent calculations, the plasma concentration oscillations near the ionosphere determining the TEC oscillations registered by the GPS receiver system, are mainly linked to the longitudinal velocity component of the oscillations (31). Therefore, having the linearized Eq. (21) retain the main term only, $\sim v_{\parallel}$, that has an antinode in the ionospheric conductive layer, produces the following expression for the disturbed density

$$\tilde{\rho} \approx i\frac{v_{\parallel}}{\omega\sqrt{g_1 g_2}}\frac{\partial}{\partial \ell}\rho_0\sqrt{g_1 g_2}, \quad (32)$$

which serves as a basis for determining the plasma concentration oscillations.

3. Determination of standing SMS wave components using the WKB approximation

In order to obtain a qualitative picture of the structure of the main components of the SMS oscillation field under consideration, let us solve the Eq. (22) in the WKB approximation. Its solution may be found using perturbation theory methods. In the zero order we obtain Eq. (22), and we use (20) as the boundary condition, where we assume the ionosphere to be ideally conductive ($\Sigma_P^{(-)} \to \infty$). This is similar to the vanishing of the tangential components of the oscillation electric field: $E_1(x^1,\ell_{\pm}) = E_2(x^1,\ell_{\pm}) = 0$. Hence we have $H(x^1,\ell_{\pm}) = 0$, where $\ell_{\pm}$ are the intersection points of a field line with the upper boundary of the ionospheric conducting layer in the Northern (plus) and Southern (minus) hemispheres, respectively. In the first order of the perturbation theory it is possible to obtain an equation for the function $V(x^1)$, and to take into account the nonzero right part in the boundary condition (20). Solving this equation it is possible to determine the amplitude distribution of $V(x^1)$, expressed through the amplitude of external currents in the ionosphere. The procedure is presented in its full form in Kozlov (2008). Unfortunately we do not know the amplitude of external currents in the ionospheric conducting layer. Therefore we will restrict ourselves to solving the zero approximation describing longitudinal eigenfunctions $H(x^1,\ell)$. We will determine the TEC oscillation amplitude applying the data on the parallel plasma velocity of the oscillations, registered by the DEMETER satellite simultaneously with TEC oscillations, to calibrating the eigenfunctions.

The solution of (22), with such boundary conditions, is a series of eigenfunctions $H_n(x^1,\ell)$ and corresponding eigenfrequencies $\Omega_{Sn}(x^1)$, where $n=1,2,3,\ldots$ is the longitudinal wavenumber. In the two first orders of the WKB approximation the solution of (22) satisfying the above boundary conditions has the form

$$H_n = C_n\sqrt{\frac{\alpha C_s}{\Omega_{Sn}}}\sin\left(\Omega_{Sn}\int_{\ell_-}^{\ell}\frac{d\ell'}{C_s}\right), \quad (33)$$

where C_n is an arbitrary constant, $\Omega_{Sn} = \pi n/t_s$,

$$t_s = \int_{\ell_-}^{\ell_+}\frac{d\ell'}{C_s} \quad (34)$$

is the travel time at SMS wave velocity along a field line between the magnetoconjugate ionospheres.

Thus, the form of the solution (33) implies that it is only those components of the standing SMS wave field that have an antinode in the ionospheric conductive layer ($\sim \nabla_3\psi_S \sim \partial\psi_S/\partial\ell$) that will have an amplitude large enough to be observed near the ionosphere. It is clear from (25)–(32) that $\mathbf{B}_{\perp} = (B_1/\sqrt{g_1}, B_2/\sqrt{g_2})$, $v_{\parallel}$ and $\tilde{\rho}$ are such field components. For the n-th harmonic of standing SMS waves we have, in the WKB-approximation,

$$v_{\parallel n} = \frac{w_n}{\rho_0}\sqrt{\frac{\alpha}{C_s}}\cos\left(\Omega_{Sn}\int_{\ell_-}^{\ell}\frac{d\ell'}{C_s}\right),$$

where the notations are $w_n(x^1) = C_n V_n(x^1) ck_2^2/4\pi\Omega_{Sn}^{3/2}(x^1)$. Plasma density disturbance is determined by Eq. (32) when $v_{\parallel} = v_{\parallel n}$ and $\omega = \Omega_{Sn}$, while for the main component of a disturbed magnetic field of azimuthally small-scale SMS waves we have

$$B_{\perp} \approx B_y = B_2/\sqrt{g_2} = v_{\parallel n}\Omega_{Sn}B_0\sqrt{g_2}/k_2A^2.$$

Let us now address the results of numerical calculations of the spectrum and structure of basic field components of standing SMS waves.

4. Numerical calculation results and discussion

The calculations below refer to the date of June 14, 2008, discussed in Afraimovich et al. (2009), when the TEC oscillations related to the terminator transit in the magnetoconjugate ionosphere were observed over Japan. The field line crossing the Northern hemisphere at the point with coordinates (37°N, 138°E) is taken as an example. The numerical model of Krinberg and Taschilin (1984) was used to calculate the medium parameters. The numerical calculations relied on a coordinate system (a,ϕ,θ) associated with the field line of a dipole magnetic field (see Fig. 1). Here a is the equatorial radius of a field line, ϕ is the azimuthal angle, θ is the latitude measured from the equator. The radius vector of a point on a field line in this coordinates system is

$$r = a\cos\theta,$$

and the length element

$$dl = a\cos\theta\sqrt{1+3\sin^2\theta}\,d\theta.$$

The dipole magnetic field intensity is determined by

$$B_0(a,\theta) = \overline{B_0}\left(\frac{a_0}{a}\right)^3\frac{\sqrt{1+3\sin^2\theta}}{\cos^6\theta},$$

where $\overline{B_0}$ is magnetic field magnitude on the field line with equatorial radius a_0 (on the Earth's surface $a_0 = R_E$, $\overline{B_0} = 0.32$ G). The metric tensor components in this coordinate system are

$$g_1 = \frac{\cos^6\theta}{1+3\sin^2\theta}, \quad g_2 = a^2\cos^6\theta.$$

The $A(\theta)$ and $C_s(\theta)$ distributions along the field line in question at 11 h UT on June 14, 2008 are shown in Fig. 2.

Fig. 3 presents the diurnal variation of the periods of the first six harmonics of standing SMS waves on the field line mentioned above. One's attention is drawn to the fact that the oscillation period of the first harmonic ($\sim 300-400$ min) is very different from those of all the other harmonics (less than 90 min). As was expected, the difference between the oscillation periods calculated both numerically and in the WKB approximation decreases with the harmonic number n. The range of the TEC oscillation periods observed in Afraimovich et al. (2009) includes harmonics with $n=4,5,6$. Given the fact that oscillations with periods larger than 30 min were filtered in the observations, one can expect lower-frequency harmonics to be present as well. However, they are difficult to extract against the background of dynamical effects related to the motion of the GPS satellites.

Fig. 4 presents the structure of $H_n(\theta)$ for the four first harmonics of standing SMS waves on the field line under consideration at 11 h UT on June 14, 2008. One can see that the structures of the first harmonic calculated numerically and in the

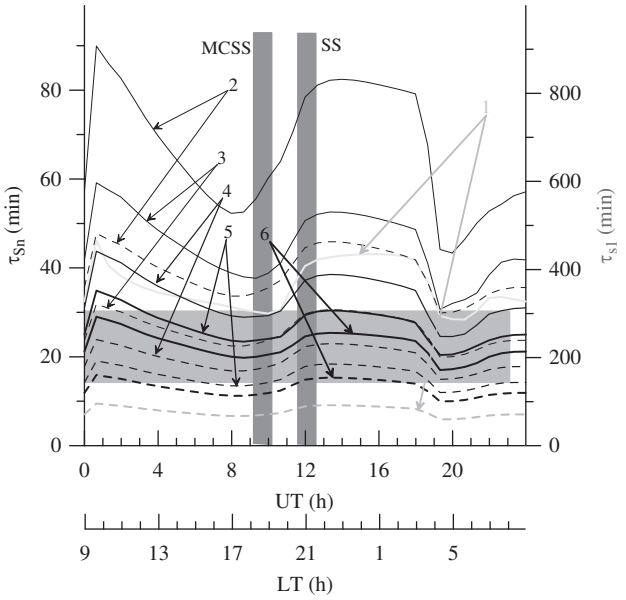

Fig. 3. Diurnal variation of the oscillation periods of the first six harmonics of standing SMS waves on June 14, 2008 for the field line crossing the ionosphere at (37°N, 138°E). The dashed lines denote the oscillation periods in the WKB approximation, the solid lines show the periods from the numerical solution of the Eq. (22). The oscillation period of the first harmonic τ_{s1} is shown in grey (vertical axis to the right). The horizontal grey band is the range of the periods of the TEC oscillations observed in Afraimovich et al. (2009). The vertical grey bands are the characteristic times of the terminator transit at the observing point (SS) and at the magnetoconjugate point (MCSS).

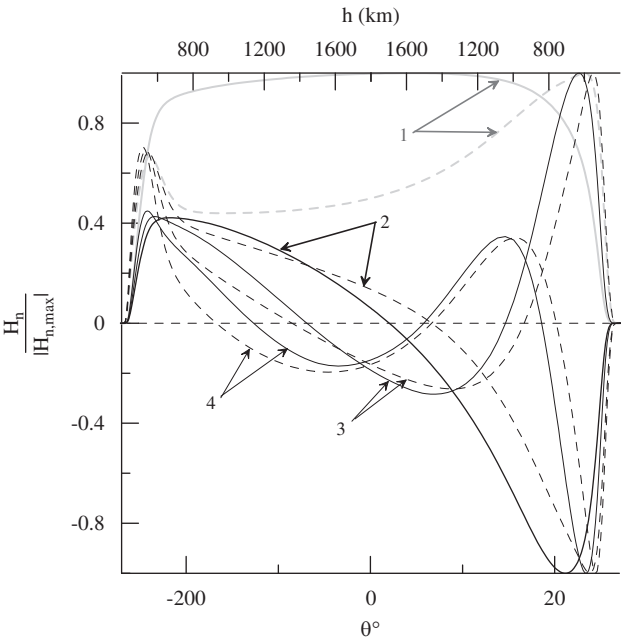

Fig. 4. Structure of the first four harmonics of standing SMS waves along the field line crossing the ionosphere at (37°N, 138°E) at 11 h UT on June 14, 2008. The dashed lines present the structure of the oscillation field in the WKB approximation, solid lines show the structure as obtained by numerically solving the Eq. (22).

WKB approximation differ very much. The structures of higher harmonics are not so different, the difference decreasing with harmonic number n. Fig. 5 presents the structure of derivatives $dH_n/d\theta$ for the 4th, 5th, 6th harmonics, which are within the frequency band of the oscillations observed in Afraimovich et al. (2009). Note that these derivatives, defining the structure of the

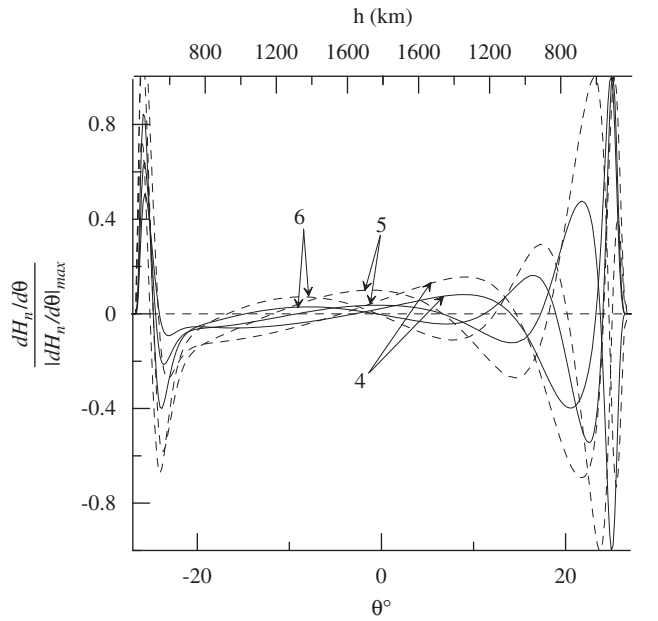

Fig. 5. Structure of derivatives $dH_n/d\theta$ for the 4th, 5th, 6th harmonics of standing SMS waves on the field line crossing the ionosphere at (37°N, 138°E) at 11 h UT on June 14, 2008. The dashed lines present the structure of the oscillation field in the WKB approximation, solid lines show the structure obtained by numerically solving the Eq. (22).

SMS wave field components near the ionosphere, have rather sharp peaks at altitudes $\sim 200-400$ km. This fact is important for the technique for estimating the TEC oscillations which is presented below.

To find the standing SMS wave amplitude distribution it is necessary to specify the amplitude of a component of the waves at any point on the field line. The most direct way is to specify the oscillation amplitude in the regions of the source—terminator transit over the ionosphere. Unfortunately, there are still no direct measuring of such oscillations simultaneously with observations of the TEC oscillations in the magnetoconjugate ionosphere. There is a work by Onishi et al. (2009), however, providing data on simultaneous observations of the TEC oscillations and the longitudinal velocity component of the plasma oscillations $v_\parallel$ by the DEMETER satellite, flying over the region of the TEC oscillations at altitudes of 650–700 km. One cannot be completely sure, of course, that the oscillations observed in Onishi et al. (2009) are standing SMS waves, but we will still make an attempt to apply the relations in that work to calibrating the SMS oscillations we are now discussing. During several passages over North America, the DEMETER satellite registered $v_\parallel$ oscillations with amplitudes 20–80 km/s and the accompanying TEC oscillations with amplitudes $(0.1–0.6)\times 10^{16}\,\mathrm{m}^{-2}$ (oscillations of the total electron content in a tube $1\,\mathrm{m}^2$ in cross-section running from the satellite to the GPS receiver on the Earth's surface).

We will set the oscillation amplitude $|v_\parallel| = 50$ km/s at altitude 660 km in our subsequent calculations. Let us assume that the spectrum of the observed oscillations is dominated by oscillations of a certain harmonic, so that the set amplitude of $v_\parallel$ determines the oscillations of this particular harmonic. Fig. 6 presents the distribution of $v_\parallel$ along the magnetic field line for the 4th, 5th, 6th harmonics of standing SMS waves. The different signs of $v_\parallel$ correspond to antiphase oscillations. The most interesting feature of these oscillations is a sharp growing amplitude, by several orders of magnitude, at altitudes $h < 400$ km. As follows from (31), this is due to a sharp decrease in ρ_0 (see also Fig. 2). Of course, the

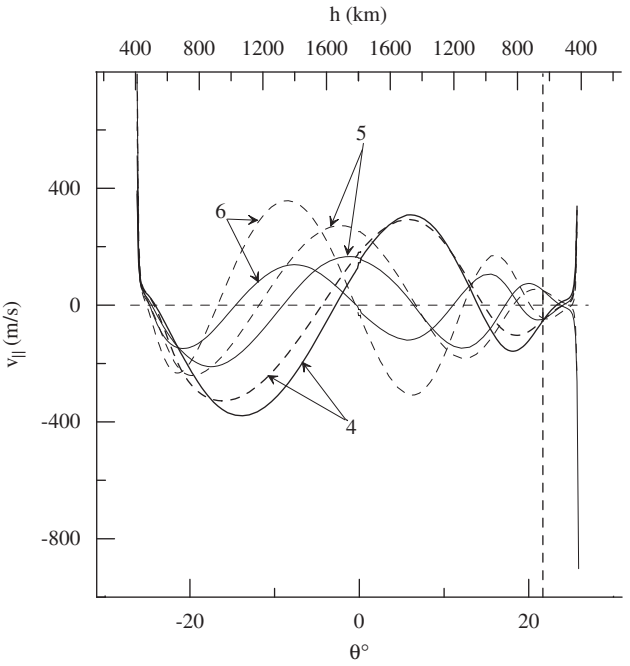

Fig. 6. Distribution of the longitudinal velocity component $v_{\parallel}(\theta)$ for the 4th, 5th, 6th harmonics of standing SMS waves along the field line crossing the ionosphere at (37°N, 138°E) at 11 h UT on June 14, 2008. The dashed curves are the amplitude distribution in the WKB approximation, the solid lines show the amplitude of $v_{\parallel}(\theta)$ obtained by numerically solving the Eq. (22). The dashed vertical line is the altitude of calibrating $v_{\parallel}$ based on satellite data in Onishi et al. (2009) ($|v_{\parallel}| = 50$ km/s at altitude $h = 660$ km.)

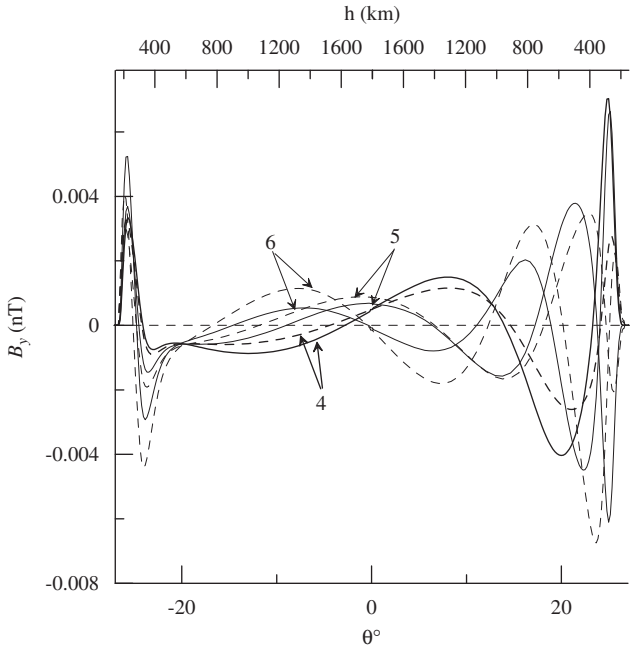

Fig. 7. Distribution of the main component ($B_y(\theta)$) of the oscillation magnetic field under consideration with the azimuthal wave number $m=20$ for the 4th, 5th, 6th harmonics of standing SMS waves along the field line crossing the ionosphere at (37°N, 138°E) at 11 h UT on June 14, 2008. The dashed curves present the distribution of $B_y(\theta)$ in the WKB approximations, the solid lines show $B_y(\theta)$ as obtained by numerically solving the Eq. (22).

model medium in this work does not include the influence of medium viscosity and collisions between charged particles and neutrals. In the real ionosphere, therefore, the oscillation amplitude will not increase so dramatically, but still it may be asserted that the increase will be rather significant. This in turn should result in charged particles periodically precipitating into the ionospheric F2 region, possibly accompanied by an airglow of the neutral component at these altitudes. If the terminator transit in the magnetoconjugate ionosphere is regarded as a possible source of such oscillations, the pre-dawn 1–2 h at a time close to the winter solstice should be the most favourable times for observing the airglow. It is during this time that the delay between the passage of the terminator through the Northern hemisphere and through the magnetoconjugate area in the ionosphere of the Southern hemisphere is longest.

Let us consider now the distribution of the amplitude of the longitudinal component of the oscillation magnetic field along a field line. Fig. 7 shows the amplitude distribution of the B_y−component of the field ($B_y = B_2/\sqrt{g_2}$ is a physical component), which is the predominant component near the ionosphere, for the 4th, 5th, 6th harmonics of standing SMS waves. It follows from (11) that the amplitude of the component is inversely proportional to the azimuthal wave number m. Estimating the typical width of the terminator front $\sim 1-2$ h, we choose $m=20$. The plots demonstrate that the amplitude reaches its maximum at altitudes $h<400$ km and does not exceed 0.008 nT. This means that the magnetic field oscillations are almost impossible to extract against the background of natural noise.

Finally, let us consider electron density oscillations in standing SMS waves. In the model medium we employ, the plasma consists of several types of ions. In the ideal MHD approximation used for calculating the structure of standing SMS waves, the density of quasi-neutral plasma is calculated as $\tilde{\rho} = \tilde{m}\tilde{n}$, where

$$\tilde{n} = \sum_i n_i$$

is total ion concentration,

$$\tilde{m} = \frac{\sum_i n_i m_i}{\sum_i n_i}$$

is normalised mass of the plasma particles, and the summing is for all the particle types. It follows from (32) that the above calculation of $v_{\parallel}$ determines the distribution of $\tilde{\rho}$, that together with a quasi-neutrality condition of plasma result in $n_e = \tilde{n} = \tilde{\rho}/\tilde{m}$—the disturbance of the electron concentration.

Fig. 8 presents the distribution of n_e along the field line for the 4th, 5th, 6th harmonics of standing SMS waves. n_e exhibits sharp peaks at altitudes ~ 200 km in the Southern hemisphere and at ~ 300 km in the Northern hemisphere. This fact enables us to estimate the magnitude of the TEC oscillations by integrating n_e along a magnetic field line. Thanks to a sharp peak in the n_e distribution, the magnitude of

$$N_{e\parallel}(\theta) = \int_{\ell_\pm}^{\ell} n_e d\ell' = a\int_{\theta_\pm}^{\theta} n_e(\theta')\cos\theta'\sqrt{1+3\sin^2\theta'}\,d\theta',$$

at altitudes $h>400$ km should not be much different from the TEC oscillation amplitudes obtained by integrating along the line drawn from the GPS receiver on the Earth's surface to the satellite. Here the $\pm$ signs refer to the upper boundary of the ionospheric conductive layer in the Northern and Southern hemispheres, respectively, and integration is along the magnetic field line.

Fig. 9 presents the distribution of $N_{e\parallel}(\theta)$ in the Southern and Northern parts of the plasmasphere for the 4th, 5th, 6th harmonics of standing SMS waves. It is evident that the thus-obtained oscillation amplitudes $|N_{e\parallel}| \sim (0.4-0.8)\times 10^{16}\,\mathrm{m}^{-2}$ for $h>400$ km, tally well with the TEC oscillation amplitudes observed in Onishi et al. (2009). This makes us hope that the oscillations observed in Onishi et al. (2009) are also SMS

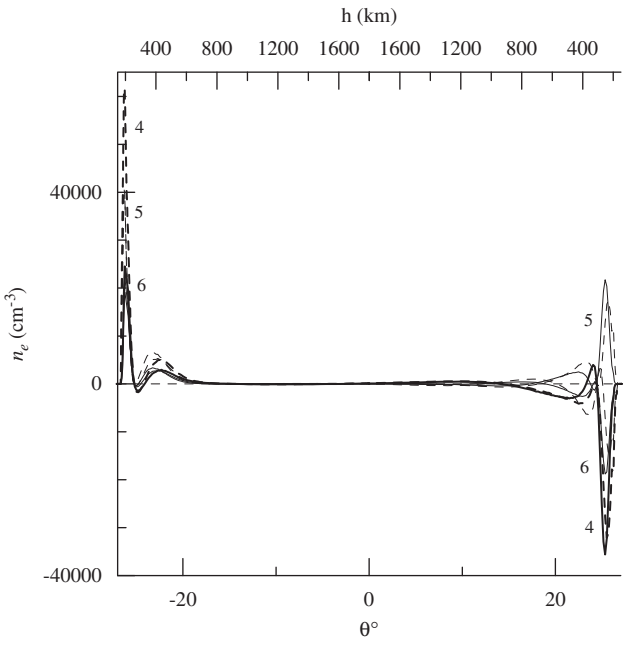

Fig. 8. Distribution of the electron concentration $n_e(\theta)$ oscillations for the 4th, 5th, 6th harmonics of standing SMS waves along the field line crossing the ionosphere at (37°N, 138°E) at 11 h UT on June 14, 2008. The dashed curves present the distribution of $n_e(\theta)$ in the WKB approximation, the solid lines show $n_e(\theta)$ as obtained by numerically solving the Eq. (22).

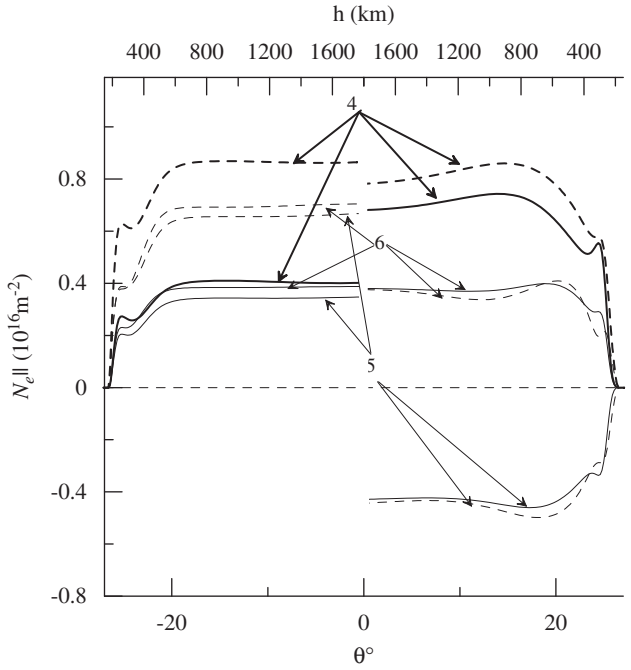

Fig. 9. Distribution of the total electronic content $N_{e\|}(\theta)$ for the 4th, 5th, 6th harmonics of standing SMS waves along the field line crossing the ionosphere at (37°N, 138°E) at 11 h UT on June 14, 2008. The dashed curves present the distribution of $N_{e\|}(\theta)$ in the WKB approximation, the solid lines show $N_{e\|}(\theta)$ as obtained by numerically solving the Eq. (22).

oscillations. TEC oscillation amplitudes observed in Afraimovich et al. (2009) are 10 times as small $(0.01–0.04) \times 10^{16}\,\mathrm{m}^{-2}$.

It follows from the above said that near the ionosphere it is the oscillations of the longitudinal component of plasma velocity $v_\|$ and plasma concentration $\tilde{n}$ oscillations (and relevant TEC oscillations) that are the observable parameters of standing SMS waves. Notably, it follows from (32) that the oscillations of $v_\|$ and $\tilde{n}$ are $\pi/2$ out of phase at any point. However, this dephasing may be different for unsteady oscillation.

5. Conclusion

Let us list the main results of this study.

1. The Eq. (22) is obtained for calculating the field structure of azimuthally small-scale standing SMS waves in a dipole-like plasmasphere. Both an analytical (WKB) and numerical solutions are obtained to this equation for the plasma parameters distributed similarly to the Earth's plasmasphere.
2. The spectrum of the oscillation periods of the first harmonics of standing SMS waves is calculated on the field line crossing the Earth's ionosphere at (37°N, 138°E) at 11 h UT on June 14, 2008. Of the harmonics we have calculated, the 4th, 5th and 6th harmonics fall within the range of periods of the observed oscillations treated in Afraimovich et al. (2009) as standing SMS waves.
3. Longitudinal (along the above-mentioned magnetic field line) distributions have been plotted for the components of the SMS wave field ($v_\|$, n_e, B_y) that can be observed near the ionosphere at the low-orbit DEMETER satellite. It is shown that near the ionosphere, the field of standing SMS waves are plasma oscillations along the background magnetic field, which do not perturb this field. The plasma velocity $v_\|$ and plasma concentration $\tilde{n}$ oscillations are $\pi/2$ out of phase at any point.
4. Calibration of the amplitudes of the above field components in the numerical calculations relied on the data of simultaneous observations of the TEC oscillations and the $v_\|$ oscillations by the DEMETER satellite in Onishi et al. (2009). The TEC oscillations $N_{e\|} \sim (0.4-0.8) \times 10^{16}\,\mathrm{m}^{-2}$ calculated by us for the 4th, 5th, 6th harmonics of standing SMS waves are in good agreement with TEC oscillations $N_e \sim (0.1-0.6) \times 10^{16}\,\mathrm{m}^{-2}$ observed by Onishi et al. (2009).

Acknowledgements

The authors are grateful to A.V. Tashchilin and L.A. Leonovich for computing the background plasma parameters that we used in our numerical calculations. This work was partially supported by RFBR Grant #09-02-00082 and by Program of presidium of Russian Academy of Sciences #4 and OFN RAS #15.

References

Afraimovich, E.L., Edemskiy, I.K., Leonovich, A.S., Leonovich, L.A., Voeykov, S.V., Yasyukevich, Y.V., 2009. MHD nature of night-time MSTIDs excited by the solar terminator. Geophys. Res. Lett. 36, L15106. doi:10.1029/2009GL039803.

Chen, L., Cowley, S.C., 1989. On field line resonances of hydromagnetic Alfven waves in a dipole magnetic field. Geophys. Res. Lett. 16, 895–897.

Cummings, W.D., O'Sullivan, R.L., Coleman, P.J., 1969. Standing Alfven waves in the magnetosphere. J. Geophys. Res. 74, 778–786.

Klimushkin, D.Yu., Mager, P.N., 2008. On the spatial structure and dispersion of slow magnetosonic modes coupled with Alfven modes in planetary magnetospheres due to field line curvature. Planet. Space Sci. 56, 1273–1279.

Korn, G.A., Korn, T.M., 1968. Mathematical Handbook for Scientists and Engineers. McGraw-Hill Book Company, New York.

Kozlov, D.A., 2008. Slow magnetosonic oscillations with $m \gg 1$ in a dipole magnetosphere with rotating plasma. Int. J. Geomagn. Aeron. 7, GI3004. doi:10.1029/2006GI000164.

Krinberg, I.A., Taschilin, A.V., 1984. Ionosphere and Plasmosphere (in Russian). Nauka, Moscow.

Lee, D.-H., Lysak, R.L., 1991. Monochromatic ULF wave excitation coupling in the dipole magnetosphere. J. Geophys. Res. 96, 5811–5823.

Leonovich, A.S., Mazur, V.A., 1989. Resonance excitation of standing Alfven waves in an axisymmetric magnetosphere (monochromatic oscillations). Planet. Space Sci. 37, 1095–1108.

Leonovich, A.S., Kozlov, D.A., Pilipenko, V.A., 2006. Magnetosonic resonance in a dipole-like magnetosphere. Ann. Geophys. 24, 2277–2289.

Leonovich, A.S., Kozlov, D.A., 2009. Alfvenic and magnetosonic resonances in a nonisothermal plasma. Plasma Phys. Controlled Fusion 51, 085007. doi:10.1088/0741-3335/51/8/085007.

Onishi, T., Tsugawa, T., Otsuka, Y., Berthelier, J.-J., Lebreton, J.-P., 2009. First simultaneous observations of daytime MSTIDs over North America using GPS-TEC and DEMETER satellite data. Geophys. Res. Lett. 36, L11808. doi:10.1029/2009GL038156.

Pilipenko, V.A., Fedorov, E.N., 1995. Modulation of total electron content in the ionosphere by geomagnetic pulsations. Geomagn. Aeron. 34, 516–519.

Radoski, H.R., 1967. Highly asymmetric MHD resonances. The guided poloidal mode. J. Geophys. Res. 72, 4026–4033.

Taylor, J.P.H., Walker, A.D.M., 1987. Theory of magnetospheric standing hydromagnetic waves with large azimuthal wave number. 2. Eigenmodes of magnetosonic and Alfven oscillations. J. Geophys. Res. 92, 10046–10052.

Wright, A.N., 1992. Coupling of fast and Alfven modes in realistic magnetospheric geometries. J. Geophys. Res. 97, 6429–6438.